This is the accepted manuscript made available via CHORUS. The article has been published as:

Three-dimensional non-Abelian anyons: Degeneracy splitting and detection by adiabatic cooling

Seiji J. Yamamoto, Michael Freedman, and Kun Yang

Phys. Rev. B **84**, 104503 — Published 6 September 2011

DOI: 10.1103/PhysRevB.84.104503

3D Non-Abelian Anyons: Degeneracy Splitting and Detection by Adiabatic Cooling

Seiji J. Yamamoto,[1] Michael Freedman,[2] and Kun Yang[1]

[1]*National High Magnetic Field Laboratory and Department of Physics, Florida State University, Tallahassee, Florida 32306, USA*

[2]*Microsoft Research, Station Q, Elings Hall, University of California, Santa Barbara, CA 93106, USA*

(Dated: August 11, 2011)

Three-dimensional non-Abelian anyons have been theoretically proposed to exist in heterostructures composed of type II superconductors and topological insulators. We use realistic material parameters for a device derived from Bi_2Se_3 to quantitatively predict the temperature and magnetic field regimes where an experiment might detect the presence of these exotic states by means of a cooling effect. Within the appropriate parameter regime, an adiabatic increase of the magnetic field will result in a decrease of system temperature when anyons are present. If anyons are not present, the same experiment will result in heating.

PACS numbers: 07.20.Mc, 05.30.Pr, 65.40.gd, 74.25.Uv

I. INTRODUCTION

Majorana fermions (which are responsible for the non-Abelian content of Ising anyons[1]) have been proposed to exist in a number of condensed matter settings. One particularly intriguing development involves the Majorana states trapped within the hedgehog defects that emerge at the interface between a topological insulator and the mouths of vortices in a type II superconductor[2]. Since the realization of anyon statistics is generally believed to be impossible beyond two dimensions, the novelty of this setup is its three dimensional (3D) nature. The paradox resolves upon realizing that the anyons at hedgehogs are not merely point-like objects, but singularities of a $U(n)/O(n)$ order parameter which may be modeled by ribbons joining hedgehogs[3]. The ribbons contain additional twist degrees of freedom relevant to particle exchange: twisting a ribbon transforms the state. The anyons in the Teo-Kane model provide a projective representation of the ribbon permutation group[3]. Interestingly, this remnant of braiding in higher dimensions seems to be special to Ising anyons: Fibonacci anyons, for example, seem to have no 3D version. While these mathematical details are interesting, they are subordinate to the question relevant to physicists: Do 3D anyons really exist or are they merely theoretical constructs? To the best of our knowledge, this paper provides the first proposal to settle this question in the lab rather than via theoretical arguments.

Majorana fermions have proven challenging to unambiguously detect in any dimension not to mention the exotic 3D context we have in mind here. For example, within the setting of quantum Hall systems, relevant to 2D non-Abelian anyons, experiments usually involve edge state transport[1]. Recently, however, several *bulk* probes have been proposed[4,5]. In particular, one suggestion exploits the huge ground state degeneracy inherent to the non-Abelian anyon system to produce a cooling effect[6]. This can be understood in analogy to adiabatic cooling via spin demagnetization, but here the entropy reservoir is an anyon system rather than a spin system. Crucially, the non-Abelian entropy is temperature independent but proportional to the number of non-Abelian anyons, which, in turn, can be adiabatically (or, more precisely, isentropically) controlled by a magnetic field. Thus, an adiabatic increase in the non-Abelian entropy necessarily implies a decrease in the rest of the system's entropy. This is accomplished by a lowering of the system's temperature. While this idea has been explored in a 2D setting[6], we expect it to work even better in 3D where the topological and conventional sources of entropy (which are fundamentally 3D) will be on an equal footing.

In this paper we explore the possibility of detecting 3D anyons via cooling by applying the Teo-Kane model to a specific heterostructure involving a topological insulator and a superconductor. Since we are mainly interested in demonstrating feasibility, our principal goal will be to establish an experimentally accessible temperature window $T_L < T < T_U$ in which the cooling effect is significant. We make quantitative estimates using realistic material parameters. The upper bound of the temperature window, T_U, is determined by the temperature where sources of entropy other than anyons begin to dominate the system. The lower bound of the temperature window, T_L, is established by calculating the ground state energy degeneracy splitting that results from Majorana-Majorana tunneling. Operating at temperatures above this splitting energy allows us to treat the low energy Hilbert space as essentially degenerate.

In Section II we briefly mention existing proposals to detect the more conventional type of non-abelian Ising anyons below three dimensions. Section III describes the physical structure and material components of the device for our 3D anyon system. The model we use to analyze this device is explained in Section IV, from which we construct Majorana solutions in Section V and calculate the ground state degeneracy splitting as a function of Majorana separation in Section VI. Section VII describes the calculation of all contributions to the system entropy. We use this in Section VIII to determine the feasibility of detection by cooling and establish the parameter regime in

which to carry out the search for 3D non-abelian anyons. Our conclusions are summarized in IX.

II. MAJORANA DETECTION PROPOSALS FOR $D < 3$

There are now many proposals for condensed matter realizations of Majoranas in two dimensional systems. Among them, the most actively studied thus far is the quantum Hall state at filling factor 5/2 where detection schemes have been proposed using both edge[7,8] and bulk[4,5] probes. Some tantalizing evidence has been reported based on the former[9,10]. Other systems in which Majoranas may exist and detection strategies have been theoretically proposed include strontium ruthenates[11], helium-3[12], topological insulator based heterostructures[13], semiconductor heterostructures[14,15], cold atoms systems[16], and quantum wire networks[17–20]. The experimental confirmation of the existence of these 2D Majoranas has lagged somewhat the large number of theoretical propositions.

Nonetheless, all these Majorana fermions are of the two dimensional $SU(2)_2$ Ising anyon variety[1]. They are representations of the braid group. The possibility for anyons beyond two dimensions came as a bit of a shock[21,22] due to certain long-standing trusted mathematical arguments. It turns out that no mathematical theorems need to be corrected because these 3D anyons do not provide representations of the braid group but rather provide projective representations of the ribbon permutation group[3].

We also mention in passing that the quantum wire networks involve 1D Majorana fermions in a sense, but their braiding (for example using T-junctions as proposed by Alicea et al[20]) still requires the spanning of 2D real space by the network. Furthermore, these 1D Majoranas are still linked to the 2D anyon statistics tied up with the braid group rather than the 3D projective ribbon permutation statistics of 3D anyons.

III. DEVICE STRUCTURE AND MATERIALS

Consider an s-wave, type II superconductor sandwiched between layers of a 3D topological insulator. The superconductor occupies the region $-\frac{L}{2} < z < \frac{L}{2}$ with flanking layers of topological insulator for $\frac{L}{2} < |z| < L$. This structure is repeated along the $\hat{z}$-direction to build a superlattice and thus a true bulk 3D system. See figure 1. Due to this periodicity, our calculations will only need to consider a single superlayer. For the topological insulator, we choose Bi_2Se_3 appropriately p-doped so that the Fermi level (ϵ_F) is pushed down into the bulk gap. For the superconductor, we choose the n-doped material $Cu_{0.12}Bi_2Se_3$ which is known to be a strongly type II ($\kappa = \lambda/\xi \approx 50$) bulk superconductor[23]. The precise nature of the superconductivity in this material is not yet known, but a theoretical proposal has suggested that it may be unconventional[24]. In the absence of further experimental data, we will assume it to be s-wave; this and other caveats are discussed further at the end of the paper.

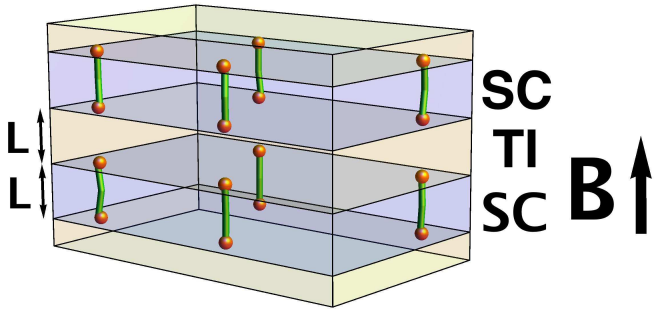

FIG. 1: (color online) Two superlayers of the heterostructure consisting of alternating layers of topological insulator (TI) and superconductor (SC). The external magnetic field induces vortices (green tubes) in the SC layers that terminate at the interface with the TI layers resulting in 3D anyons (orange balls). In addition to the obvious three dimensional distribution of anyons in real space, these anyons provide a projective representation of the ribbon permutation group[3] which further distinguishes them from the more well-known two dimensional anyon system (which forms a representation of the braid group).

Existing experimental results on $Cu_{0.12}Bi_2Se_3$ (almost) supply the required minimal input needed for our calculation. ARPES provides numbers for the Fermi energy, velocity, wavevector, and the spin-orbit gap[25]: $\epsilon_F = 400$ meV, $\hbar v_F = 3.8$ eV Å, $k_F = 0.1$ Å^{-1} $\approx \epsilon_F/\hbar v_F$, and $\Delta_{so} = 150$ meV. We also need the superconducting gap (Δ) and coherence length (ξ). Based on the existing experimental data, there are two ways of determining Δ and ξ. Both quantities could be inferred from the known superconducting transition temperature, $T_c = 3.8$ K[23], using the BCS relations $\Delta = 1.764 k_B T_c$ and $\xi = \hbar v_F/\pi\Delta$. On the other hand, we could use the measurement of the upper critical field, $B_{c2} = 1.7$ Tesla[23], to give a more direct estimate of the coherence length $\xi = \sqrt{\frac{h/2e}{2\pi B_{c2}}} \approx 139$ Å independent of BCS theory. This could then be combined with the BCS relation $\Delta = \hbar v_F/\pi\xi$ to give a value for the superconducting gap. The fact that these two methods do not agree[23,25] provides a puzzle for the community. What is needed is a *direct* measurement of Δ, which has not been reported yet. Since this paper is chiefly concerned with vortices we will trust the B_{c2}-derived value of ξ, which is 139 Å. To be consistent, this value of ξ is then used to set $\Delta = 8.7$ meV.

Very recently, another indirect estimate of the gap has been made using specific heat data[26]. Weak-coupling BCS theory does not fit the data, while a fit to strong-coupling BCS theory produces parameter values inconsistent with other measures. Therefore, the main conclusions to be drawn from this experiment are the bulk

nature of the superconductivity, the lack of nodes in the gap, and the fact that the gap is larger than would be expected from BCS theory using T_c. We therefore continue to use B_{c2} to estimate the value of the superconducting gap.

IV. THEORETICAL MODEL

The low-energy theory is an eight-band Dirac model[2,27,28]: $H = \frac{1}{2}\int d^3x \Psi^\dagger \mathcal{H} \Psi$ where

$$\mathcal{H} = \begin{pmatrix} \mathcal{H}_D & \Delta \\ \Delta^* & -\mathcal{H}_D \end{pmatrix} \quad (1)$$

with diagonal terms given by $\mathcal{H}_D = \boldsymbol{\alpha}\cdot\mathbf{p} - \epsilon_F - i\gamma^5\beta\Delta_{so}$. We use the standard Dirac-Pauli representation: $\boldsymbol{\alpha} = \begin{pmatrix} 0 & \boldsymbol{\sigma} \\ \boldsymbol{\sigma} & 0 \end{pmatrix}$, $\beta = \begin{pmatrix} \mathbb{1} & 0 \\ 0 & -\mathbb{1} \end{pmatrix}$, $\gamma^5 = \begin{pmatrix} 0 & \mathbb{1} \\ \mathbb{1} & 0 \end{pmatrix}$. The fermion is an eight-component object deriving from spin, orbital, and particle-hole degrees of freedom: $\Psi^\dagger = \left(\psi^\dagger, -i\psi^T\alpha_2\right) = (u_1^\dagger, u_2^\dagger, v_2^\dagger, v_1^\dagger)$, where each u_i and v_i has two components. Particle-hole symmetry enforces $v_i = i\sigma_2 u_i^*$. We have written the model in the same way as Ref. 27, which is unitarily equivalent to the models used in Refs. 2 and 28. Variants of this model have been studied for many years[29].

We use a Dirac Bogoliubov-de-Gennes (BdG) model for this material. The construction of the effective model for Bi_2Se_3 has been discussed by several groups, see for example[30] and references therein. While higher momentum terms can sometimes lead to interesting physics, the situation we are considering only requires use of a Dirac model.

V. MAJORANA SOLUTIONS

We combine the superconducting and spin-orbit gaps into a single 3-component order parameter[2]: $\vec{n} = (\mathrm{Re}\Delta, \mathrm{Im}\Delta, \Delta_{so})$. Within the superconductor, a vortex excitation along the z-axis is achieved by imposing the following profile on the superconducting order parameter: $\Delta(\rho,\theta,z) = \Delta(\rho)e^{in\theta}\Theta(L/2-|z|)$. The interface between the topological insulator and superconductor is specified by imposing the following kink profile on the spin-orbit gap: $\Delta_{so}(\rho,\theta,z) = +\Delta_{so}$ for $|z| \ll L/2$ and $\Delta_{so}(\rho,\theta,z) = -\Delta_{so}$ for $|z| \gg L/2$. In this way the band is inverted within the topological insulator, while taking the opposite sign in the (topologically trivial) superconductor. Note that we have considered a topological insulator and trivial superconductor, but the kink would also exist at the interface of a trivial insulator and a topological superconductor.

The combination of a vortex in Δ and a Z_2 kink in Δ_{so} leads to an anisotropic hedgehog in $\vec{n}$ occurring where the vortex tube meets the interface with the topological insulator. We can think of this defect as a potential well and solve for the zero energy solutions of the BdG equation $\mathcal{H}\Psi = 0$. At the kink ($z = -L/2$) this leads to the following Majorana zero-mode wavefunctions[27,28]

$$\begin{pmatrix} u_{1\uparrow} \\ u_{1\downarrow} \\ u_{2\uparrow} \\ u_{2\downarrow} \end{pmatrix} = \mathcal{N} \begin{pmatrix} J_{(n-1)/2}(k_F\rho)\, e^{-i\pi/4} e^{i(n-1)\theta/2} \\ 0 \\ 0 \\ J_{(n+1)/2}(k_F\rho)\, e^{i\pi/4} e^{i(n+1)\theta/2} \end{pmatrix} \times\sqrt{\epsilon_F} e^{-\frac{1}{\hbar v_F}\int^\rho \Delta(\rho')d\rho'} e^{-\frac{1}{\hbar v_F}\int^z \Delta_{so}(z')dz'} \quad (2)$$

while at the upper interface ($z = L/2$) we have an anti-kink given by cyclically permuting the right hand side two steps. The expressions for v_i follow from particle-hole symmetry and $\mathcal{N}$ is a normalization constant given by $\mathcal{N}^2 = \frac{\epsilon_F}{2\hbar^2 v_F^2 \xi_z [E(-\epsilon_F^2/\Delta^2) - K(-\epsilon_F^2/\Delta^2)]}$ where K and E are the complete elliptic integrals of the first and second kinds. These expressions are valid inside the superconductor. We ignore the exponential tail decaying into the topological insulator which is miniscule due to the large insulating gap.

An exact treatment of this problem would numerically solve for the order parameter profiles self-consistently. See, for example, Ref. 31. However, since we desire analytical expressions we make the following standard simplification: $e^{-\frac{1}{\hbar v_F}\int^\rho \Delta(\rho')d\rho'} e^{-\frac{1}{\hbar v_F}\int^z \Delta_{so}(z')dz'} = \mathrm{sech}(\rho/\pi\xi)\mathrm{sech}(z/\xi_z)$ where $\rho \equiv \sqrt{x^2+y^2}$ and $\xi_z \equiv \hbar v_F/\Delta_{so} \approx 25.3$ Å. Thus, two experimentally determined parameters influence the localization of the Majorana wavefunction: ξ and Δ_{so} (or, equivalently, ξ_z as defined above). ξ_z determines the localization in the z-direction while ξ sets the decay length in the xy-plane. Since $\xi \gg \xi_z$, we might already speculate that the in-plane coupling between Majoranas will be much more important than the coupling in the z-direction for the degeneracy splitting. We turn to this issue next.

VI. DEGENERACY SPLITTING

With the Majorana wavefunctions in hand, we can use these expressions to calculate the splitting of the ground state degeneracy as a function of Majorana separation. This energy splitting has been calculated by a variety of means in 2D Majorana systems. We will generalize to 3D the method of Ref. 32 who adapted to 2D the 1D Lifshitz problem[33]. Our calculation is very similar to what has already been presented in Refs. 32 and 34. We refer the reader to these paper for technical details. In what follows, we outline the main idea behind the calculation.

Consider two Majorana states, Ψ_a and Ψ_b, which are brought together from infinity. As they approach each other, the degenerate eigenvalue of the two fusion channels is split by an amount E_{split}. The new eigenfunctions of this two-Majorana state are $\Psi_\pm \equiv \Psi_a \pm i\Psi_b$ with corresponding eigenvalues $E_\pm$. Particle-hole symmetry dictates $E_{\mathrm{split}} = E_+ - E_- = 2E_+$. We calculate the

eigenvalue of one of these states as follows[32]:

$$E_+ = \frac{\int_\Sigma \Psi_a^\dagger \mathcal{H}\Psi_+ - \int_\Sigma \Psi_+^\dagger \mathcal{H}\Psi_a}{\int_\Sigma \Psi_a^\dagger \Psi_+} \quad (3)$$

where Σ is an integration region corresponding to the half-infinite volume in three dimensions. The integrand can be written in terms of total derivatives, and the localized nature of the wavefunctions allows us to reduce Σ to the infinite 2d plane that bisects the line joining the two Majorana states in question. We consider two cases: vertical Majorana-Majorana coupling in the z-direction and lateral Majorana-Majorana coupling in the xy-plane.

For the vertical coupling, we place Ψ_a at $\mathbf{R}_a = (0, 0, -L/2)$ and Ψ_b at $\mathbf{R}_b = (0, 0, +L/2)$; L is the superconductor thickness. Importantly, one of these is a "kink hedgehog" while the other is an "anti-kink hedgehog." Equations (2) and (3) lead to:

$$E_{\rm split}^{(z)}(L) = E_0^{(z)} \mathrm{sech}^2\left(L/\xi_{so}\right) \quad (4)$$

$$\approx 10^{-34} \text{ eV} \quad (5)$$

where the prefactor is

$$E_0^{(z)} \equiv -\frac{4\sqrt{2}\Delta_{so}\left[K(-\epsilon_F^2/\Delta^2) - \frac{E(-\epsilon_F^2/\Delta^2)}{(1+\epsilon_F^2/\Delta^2)}\right]}{[K(-\epsilon_F^2/\Delta^2) - E(-\epsilon_F^2/\Delta^2)]} \quad (6)$$

While $E_0^{(z)}$ is seemingly a large energy scale, the sech^2 factor stemming from the in-plane localization makes the degeneracy splitting due to coupling in the z-direction completely negligible compared to what we calculate next.

For the lateral coupling within the same interface, we consider two Majoranas Ψ_a at $\mathbf{R}_a = (-R/2, 0, -L/2)$ and Ψ_b at $\mathbf{R}_b = (+R/2, 0, -L/2)$; R is the in-plane distance between hedgehogs. Unlike the case of vertical coupling, the two wavefunctions here are both kinks. Equations (2) and (3) lead to:

$$E_{\rm split}^{(xy)}(R, L) = \frac{E_0^{(xy)}(L)\cos\left(\epsilon_F R/\hbar v_F + \alpha\right)}{\sqrt{R/\xi}} e^{-\frac{R}{\pi\xi}} \quad (7)$$

where the L-dependent prefactor is

$$E_0^{(xy)}(L) \equiv \frac{8\epsilon_F \tanh(L/\xi_{so})[1 + (\epsilon_F/\Delta)^2]^{-1/4}}{[E(-\epsilon_F^2/\Delta^2) - K(-\epsilon_F^2/\Delta^2)]} \quad (8)$$

$$E_0^{(xy)}(1000\text{Å}) \approx 15 \text{ K}/k_B \quad (9)$$

and the phase shift is $\alpha \equiv (1/2)\arctan\epsilon_F/\Delta$. At the fields of interest to us, $E_{\rm split}^{(xy)}(R, L)$ is much larger than $E_{\rm split}^{(z)}(L)$, so we neglect the latter. The attenuation and period of oscillation of $E_{\rm split}^{(xy)}(R, L)$ depends on the separation between Majoranas, R, which is in turn determined by the lattice spacing of the Abrikosov vortex lattice. For a triangular lattice, this spacing is related to the field by $R = \sqrt{\frac{h/2e}{B\sqrt{3}/2}}$. Thus, the envelope of the energy splitting varies with field as $E_{\rm split}^{(xy)}(B) \propto \sqrt{B/B_0}e^{-\sqrt{B_0/B}}$, where $B_0 \equiv \frac{2h/2e}{\sqrt{3}\pi^2\xi^2} \approx 1.25$ Tesla. This sets the lower bound of the temperature window and is clearly field-dependent: $T_L(B) = E_{\rm split}^{xy}(B)/k_B$. See Fig. 3a. We next determine the upper bound of the temperature window.

VII. ENTROPY

To compute the cooling effect we need to understand all appreciable contributions to the total entropy as a function of temperature and field: $S(T, B)$. These can be classified into phonon (S_{ph}) and vortex (S_v) contributions with the latter being composed of several pieces (electronic contributions at the temperatures of interest are negligible because $\Delta, \Delta_{so} \gg k_B T$). Thus, the total entropy is given by

$$S(T, B) = S_{ph}(T) + S_v(T, B) \quad (10)$$

The phonon entropy is standard:

$$S_{ph}(T) = k_B \frac{4\pi^4 V}{5V_{uc}}\left(\frac{T}{\Theta_D}\right)^3 \quad (11)$$

where $\Theta_D \approx 182$ K is the Debye temperature of the parent compound[35] and $V_{uc} \approx 426$ Å^3 is the volume of the unit cell[23]. Within the superconductor material $Cu_xBi_2Se_3$, recent specific heat data[26] has yielded a Debye temperature of $\Theta_D \approx 120$ K.

The vortex entropy will have several contributions. The most important piece of S_v is due to the non-Abelian anyons (S_{na}); this is what drives the dramatic low-temperature cooling effect. For a large number of vortices (N_v) this is simply[6]

$$S_{na}(B) \approx N_v(B) 2k_B \log\sqrt{2}. \quad (12)$$

The non-Abelian anyon entropy only depends on B, not T, and this is through its dependence on the number of vortices: $S_{na}(B) \propto N_v(B)$ with $N_v(B) \approx BA/\phi_0$ where $\phi_0 = h/2e$ is the flux quantum and A is the sample area perpendicular to the magnetic field. This linear approximation is justified for $B \gg B_{c1}$.

The contribution to the vortex entropy from more conventional sources will depend on the vortex density, and thus the magnetic field. An isolated vortex line will contribute two types of entropy. First, there are subgap bound states that are localized to the core but extended along the z-direction. These are usually called CdGM excitations after Caroli, de Gennes, and Matricon[36]. Second, a single vortex line will have excitations analogous to those of a fluctuating string[37]. For our materials and parameter regimes, this second type of fluctuation turns out to contribute negligibly to the total entropy.

In addition to this single-vortex physics, collective effects can manifest when the magnetic field is increased

even slightly above B_{c1} leading to the formation of an Abrikosov vortex lattice. A dense array of vortices can have collective modes of the same two types as described above. First, there are collective CdGM excitations[38], and second there are modes corresponding to fluctuating elastic media[37]. Note, however, that the term "dense" must be understood with respect to the appropriate length scale. Define R as the lateral vortex-vortex distance, λ as the penetration depth, and ξ as the superconducting coherence length. Collective modes of the vortex lattice appear when the magnetic field is such that $R < \lambda$. In contrast, collective CdGM excitations only appear at the much higher density $R \sim \xi$. For our device, $B_{c1} \approx 1.3$ mT and $B_{c2} = 1.7$ T, giving a rather large range $\xi \ll R \ll \lambda$ (or, equivalently, $B_{c1} \ll B \ll B_{c2}$) in the dilute limit with respect to CdGM excitations, but the dense collective-mode limit of vortex fluctuations.

In such a regime, the CdGM entropy is given by N_v times the "isolated" vortex line contribution,

$$S_{\mathrm{CdGM}}(T,B) = \frac{N_v(B) k_B 2 k_F L}{\sqrt{2\pi}} \sqrt{\frac{g}{k_B T}} e^{-g/k_B T} \quad (13)$$

while the vortex lattice entropy takes the form[37]

$$S_{vl}(T,B) = k_B \frac{15}{8} \zeta(5/2) \left(\frac{k_B T}{\hbar \bar{\kappa} V^{-2/3}}\right)^{3/2} \left(\frac{R(B)}{\lambda}\right)^{5/2} \quad (14)$$

where $g \equiv \frac{\Delta}{2 k_F \xi}$ is the CdGM mini-gap, $\bar{\kappa} \equiv h/2m \approx 2 \times 10^{17} \text{Å}^2/s$ is the quantum of circulation, ζ is the Riemann-Zeta function, and $V = LA$ is the superconductor sample volume. This form of S_{vl}, which is proportional to $B^{-5/4}$, is only valid in the parameter regimes of interest to us. Eventually, at very low fields on the order of B_{c1}, S_{vl} must of course vanish as B decreases[37].

Thus, the total vortex entropy is given by

$$S_v(T,B) = S_{na}(B) + S_{\mathrm{CdGM}}(T,B) + S_{vl}(T,B) \quad (15)$$

When added to the phonon entropy, this yields an approximate analytic expression for the total system entropy as a function of T and B. Using these expressions we calculate the central quantity $\frac{dT}{dB} = -\frac{(dS/dB)_T}{(dS/dT)_B}$ as described in the next section.

VIII. COOLING

To understand the cooling effect, consider the small change in entropy for a system depending on temperature and field:

$$dS = \left(\frac{dS}{dT}\right)_B dT + \left(\frac{dS}{dB}\right)_T dB \quad (16)$$

For an isentropic process ($dS = 0$), the system's temperature changes in response to a small field change according to:

$$\frac{dT}{dB} = -\frac{(dS/dB)_T}{(dS/dT)_B}. \quad (17)$$

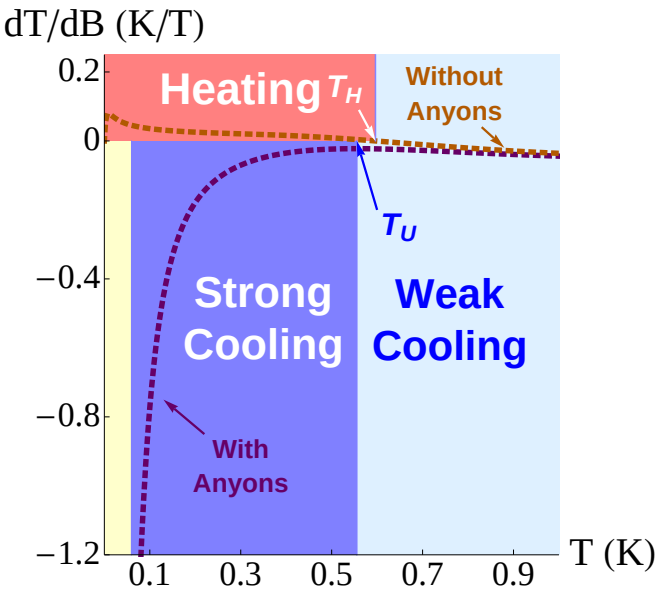

FIG. 2: (color online) Quantitative illustration of cooling via 3D non-Abelian anyons. The superconductor layer thickness is set to $L = 1000$ Å. The orange and purple dashed lines are constant field cuts ($B = 25 B_{c1} \approx 33$ mT) of $\frac{dT}{dB}$ corresponding to the orange and purple dashed lines in Fig. 3 with (a) and without (b) anyons. Notice that $T_H \gtrapprox T_U$, where T_H is defined by the temperature below which $\frac{dT}{dB} > 0$ in a system without 3D Majoranas, and T_U, the upper bound of the cooling window, is defined as the temperature below which the non-Abelian entropy strongly enhances the cooling effect in a system with 3D Majoranas.

When this quantity is negative it represents a decrease of system's temperature as the field is adiabatically increased: cooling. In contrast, a positive sign indicates heating. Importantly, the sign and magnitude of $\frac{dT}{dB}$ depend on T and B. Since $\frac{dS}{dT}$ is always positive, to find cooling we require a parameter regime in which $\frac{dS}{dB}$ is positive. This will occur when $S_{na}(B)$ dominates the total entropy.

In Fig. 2 we show the temperature dependence, both with and without 3D anyons in the system, for a fixed value of field: $B = 25 B_{c1} \gg B_{c1}$. At high temperatures dT/dB is very similar in both cases, but below a certain temperature, T_H, the system without 3D anyons will experience heating while the system with 3D anyons will experience cooling. This qualitative difference is the harbinger of 3D non-Abelian anyons.

To reiterate: weak cooling may occur at high temperatures with or without 3D anyons, but in a specific region of the BT-plane, depicted in dark blue in Fig 3a, a system with 3D anyons will exhibit strong cooling while a system without 3D anyons will experience heating (as shown in Fig 3b). For a system with 3D anyons, the transition between the strong cooling and weak cooling regimes is defined by the extremum of the curve dT/dB which is most apparent by examining the purple dashed curve in

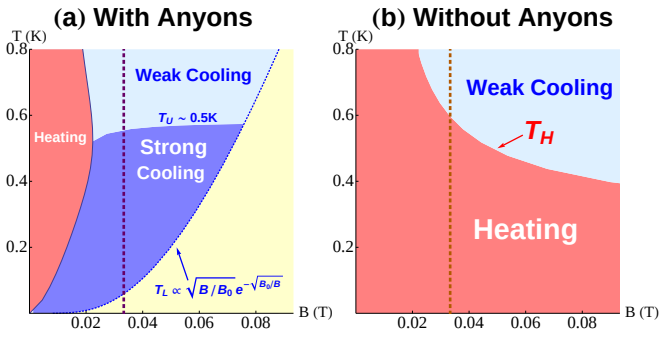

FIG. 3: (color online) Comparison of the temperature evolution with (a) and without (b) 3D non-Abelian anyons in the field-temperature plane. The superconductor layer thickness is set to $L = 1000$ Å. The sign and magnitude of $\frac{dT}{dB}(B,T)$ determines the nature of the cooling or heating effect as the magnetic field is adiabatically increased. When 3D Majoranas are present (a), a sizable temperature window $T_L < T < T_U$ at intermediate fields (darker blue region labelled "Strong Cooling") will exhibit a strong cooling effect. Without 3D Majoranas (b), the same parameter regime will demonstrate a heating effect. The yellow region below $T_L(B)$ is where the ground state degeneracy is split by Majorana-Majorana tunneling; oscillations are not shown for clarity. This interesting sector may include collective anyon excitations generalizing some ideas in 2D[39], but these are not pertinent to this paper.

Fig. 2.

To understand the origin of the minor heating without anyons note that, in the regimes relevant to our proposal, all contributions to the entropy are non-decreasing functions of B *except* S_{vl}. This part of the entropy *decreases* with field and thus dS/dB could become negative if S_{vl} were large enough compared to all the other entropy sources. Since dS/dT is always positive, the possibility of negative dS/dB means $dT/dB = -\frac{dS/dB}{dS/dT}$ could be driven positive leading to the observation of heating with an adiabatic increase of the field. Indeed, in the absence of 3D non-abelian anyons this is exactly what happens at low temperatures as depicted in Fig. 3b. However, the presence of 3D non-abelian anyons contributes S_{na} to the total entropy which increases sufficiently rapidly with B that it overwhelms the low temperature heating due to S_{vl} and reverses the trend to produce a dramatic strong cooling effect.

IX. CONCLUSION

In summary, we have quantitatively estimated a magnetic field and temperature regime in which an experiment might detect 3D non-Abelian anyons in a heterostructure device composed of Bi_2Se_3 and $Cu_{0.12}Bi_2Se_3$. Within this regime, a system with 3D non-Abelian anyons will experience a decrease in temperature as the magnetic field is adiabatically increased. In contrast, a system without 3D non-Abelian anyons under identical conditions will exhibit a temperature increase as the magnetic field is adiabatically increased. In the strong cooling region, the effect is rather large. For example, at $B = 25B_{c1}$ and $T = 0.1$ K we have $\frac{dT}{dB} \approx -1.7$ K/T, which should be detectable with present technology.

We close by enumerating a few caveats that are specific to $Cu_{0.12}Bi_2Se_3$, but not to the general idea of our proposal. First, the numbers presented in this paper are based on a value of the superconducting gap inferred from the B_{c2}-derived coherence length[23] which disagrees with the T_c derived gap[25]. Since the degeneracy splitting (*i.e.* the $T_L(B)$ line) is exponentially sensitive to this parameter, the choice is very important. We hope a direct experimental measurement of the superconducting gap will be made in the future to pin down the true value of this important parameter. Second, we have assumed the sign of Δ_{so} to take opposite values in insulating Bi_2Se_3 versus $Cu_{0.12}Bi_2Se_3$. Without the sign change, there will be no Majorana mode. Again, this needs to be experimentally checked for $Cu_{0.12}Bi_2Se_3$. Note, however, that if later experimental investigations determine that either Δ in $Cu_{0.12}Bi_2Se_3$ is much smaller than our assumption, or that Δ_{so} does not change sign in $Cu_{0.12}Bi_2Se_3$, the general idea of this proposal will not be invalidated but only its applicability to this particular superconductor; all qualitative conclusions will remain true for *any* insulator-superconductor system that satisfies the following conditions: (i) the superconductor must have a relatively large s-wave gap and be strongly type II; (ii) the band gap must take opposite signs in the insulating and superconducting regions. These are relatively simple conditions to fulfill. We chose to examine a Bi_2Se_3-based structure because this material has emerged as an archtype topological insulator which is being independently studied by many different research institutions. Furthermore, the possibility of creating topological insulator regions and superconducting regions simply by p-doping or n-doping the same parent compound makes Bi_2Se_3 a very attractive system for building heterostructure devices in the future.

X. ACKNOWLEDGEMENTS

This work is supported by DOE under Grant No. DE-FG52-10NA29659 (SJY) and NSF Grant No. DMR-1004545 (SJY and KY).

[1] C. Nayak *et al.*, Rev. Mod. Phys. **80**, 1083 (2008).
[2] J. C. Y. Teo and C. L. Kane, Phys. Rev. Lett. **104**, 046401 (2010).
[3] M. Freedman, M. B. Hastings, C. Nayak, X. L. Qi, K. Walker, and Z. Wang, Phys. Rev. B **83**, 115132 (2011).
[4] K. Yang and B. I. Halperin, Phys. Rev. B **79**, 115317 (2009).
[5] N. R. Cooper and A. Stern, Phys. Rev. Lett. **102**, 176807 (2009).
[6] G. Gervais and K. Yang, Phys. Rev. Lett. **105**, 086801 (2010).
[7] A. Stern and B. I. Halperin, Phys. Rev. Lett. **96**, 016802 (2006).
[8] P. Bonderson, A. Kitaev, and K. Shtengel, Phys. Rev. Lett. **96**, 016803 (2006).
[9] R. L. Willett, L. N. Pfeiffer, and K. W. West, Proc. Natl. Acad. Sci. **106**, 8853 (2009).
[10] R. L. Willett, L. N. Pfeiffer, and K. W. West, Phys. Rev. B **82**, 205301 (2010).
[11] S. Das Sarma, C. Nayak, and S. Tewari, Phys. Rev. B **73**, 220502 (2006).
[12] Y. Tsutsumi, T. Kawakami, T. Mizushima, M. Ichioka, and K. Machida, Phys. Rev. Lett. **101**, 135302 (2008).
[13] L. Fu and C. L. Kane, Phys. Rev. Lett. **102**, 216403 (2009).
[14] J. D. Sau, R. M. Lutchyn, S. Tewari, and S. Das Sarma, Phys. Rev. Lett. **104**, 040502 (2010).
[15] J. Alicea, Phys. Rev. B **81**, 125318 (2010).
[16] S. L. Zhu, L. B. Shao, Z. D. Wang, and L. M. Duan, Phys. Rev. Lett. **106**, 100404 (2011).
[17] A. Y. Kitaev, Phys.-Usp **44**, 131 (2001).
[18] Y. Oreg, G. Refael, and F. von Oppen, Phys. Rev. Lett. **105**, 177002 (2010).
[19] R. M. Lutchyn, J. D. Sau, and S. Das Sarma, Phys. Rev. Lett. **105**, 077001 (2010).
[20] J. Alicea, Y. Oreg, G. Refael, F. von Oppen, and M. P. A. Fisher, Nature Physics **7**, 412 (2011).
[21] C. Nayak, Nature (London) **464**, 693 (2010).
[22] A. Stern and M. Levin, Physics Online Journal **3**, 7 (2010).
[23] Y. S. Hor *et al.*, Phys. Rev. Lett. **104**, 057001 (2010).
[24] L. Fu and E. Berg, Phys. Rev. Lett. **105**, 097001 (2010).
[25] L. A. Wray *et al.*, Nat. Phys. **6**, 855 (2010).
[26] M. Kriener, K. Segawa, Z. Ren, S. Sasaki, and Y. Ando, Phys. Rev. Lett. **106**, 127004 (2011).
[27] Y. Nishida, L. Santos, and C. Chamon, Phys. Rev. B **82**, 144513 (2010).
[28] T. Fukui, Phys. Rev. B **81**, 214516 (2010), 1003.4814.
[29] R. Jackiw and C. Rebbi, Phys. Rev. D **13**, 3398 (1976).
[30] C.-X. Liu, X.-L. Qi, H. J. Zhang, X. Dai, Z. Fang, and S.-C. Zhang, Phys. Rev. B **82**, 045122 (2010).
[31] F. Gygi and M. Schlüter, Phys. Rev. B **43**, 7609 (1991).
[32] M. Cheng, R. M. Lutchyn, V. Galitski, and S. Das Sarma, Phys. Rev. B **82**, 094504 (2010).
[33] L. D. Landau and E. M. Lifshits, *Quantum Mechanics. Nonrelativistic theory* (Pergamon Press, 1974), pp. 183–184, 3rd ed.
[34] T. Mizushima and K. Machida, Phys. Rev. A **82**, 023624 (2010).
[35] G. E. Shoemake, J. A. Rayne, and R. W. Ure, Phys. Rev. **185**, 1046 (1969).
[36] C. Caroli, P. G. de Gennes, and J. Matricon, Phys. Lett. **9**, 307 (1964).
[37] A. L. Fetter, Phys. Rev. **163**, 390 (1967).
[38] E. Canel, Phys. Lett. **16**, 101 (1965).
[39] A. W. W. Ludwig, D. Poilblanc, S. Trebst, and M. Troyer, New J. of Phys. **13**, 045014 (2011).